Covariance of Meiyu Front and Tropospheric Jet Variability on Daily and Interannual time scales

Jesse A. Day,[1] Jacob Edman,[1] Inez Fung[1], and Weihan Liu[1]

————

Corresponding author: Jesse Day, University of California Berkeley, Department of Earth and Planetary Science, College of Letters and Science; 307 McCone Hall, Berkeley, CA 94720, USA. (jessed@berkeley.edu)

[1]Department of Earth and Planetary Science, University of California Berkeley, Berkeley, California, USA.

This abstract must be 150 words or less. The contents of the abstract count

towards the total word count.

1. Introduction

China receives about 60% of its rainfall from May to August, known collectively as the East Asian summer monsoon. The period of peak rainfall within this monsoon features a northward-migrating front known as the Meiyu front (lit. "Plum rains" – capitalize front?), and lasts roughly from early June to mid-July ("Meiyu Season"). A growing volume of evidence suggests a shift in mean rainfall patterns over China beginning in the late 1970s, with increased flooding in the south and droughts in the north (the "South Flood North Drought"). A permanent change would have major humanitarian impacts on the densely-populated eastern Chinese plain, where a sizable fraction of the population depends on agriculture. The Chinese government has already embarked on a costly engineering project to reroute water from the Yangtze to the Yellow River, the South-North Water Transfer Project.

The complex atmospheric dynamics of the East Asian summer monsoon remain a source of debate [*Sampe and Xie*, 2010; *Chen and Bordoni*, 2014]. The behavior of the Meiyu front has been discussed in the seasonal mean[*Ding and Chan*, 2005], and in relation to interannual rainfall variability [*Kosaka et al.*, 2011]. However, to our knowledge, no comprehensive statistics of daily Meiyu behavior exist. We have developed an algorithm to compile a 57-year climatology (1951-2007) of frontal events in China (hereafter referred to as Meiyu events) based on the APHRODITE rain gauge product. In addition, we test the covariance of daily Meiyu behavior with that of the tropospheric jet, using an existing database from *Schiemann et al.* [2009]. Past work has compared jet and Meiyu variability over shorter time periods or with coarse resolution*Liang and Wang* [1998], but

26 none has systematically compared the two. Finally, given our daily Meiyu climatology, we

27 determine whether there are apparent changes in behavior over the 57 years, and whether

28 these also correspond to changes in jet behavior.

2. Data sets

29 The analysis contained in this paper relies on two data sets, APHRODITE and Schie-

30 mann et al's database of jet counts. APHRODITE (Asian Precipitation - Highly-Resolved

31 Observational Data Integration Towards Evaluation of the Water Resources) [*Yatagai*

32 *et al.*, 2012]. The APHRO_MA_V1101 product includes 57 years (1951-2007) of daily

33 precipitation (PRECIP product, units mm day^{-1}) and station coverage (RSTN product)

34 on a .25° × .25° grid (roughly 25 km spacing) between 60°E-150°E and 15°S-55°N. We

35 focus on the subregion from 100E-123E and 20N-40N as the area of occurrence of Meiyu

36 events. Rain gauge products present an analytical challenge because the distribution of

37 stations is uneven in space and changes with time. Station density over eastern China

38 improves beginning in the 1970s from X to Y (INSERT ACTUAL NUMBERS). However,

39 the spacing of stations generally does not exceed 100 km, which should be more than

40 sufficient to resolve the macroscopic scale of a frontal event.

41 For tropospheric jet variability, we employ a database based on ERA-40 reanalysis

42 data developed by *Schiemann et al.* [2009]. Their database includes every appearance of

43 a tropospheric jet in East Asia for 1958-2001 at 6-hourly intervals using simple criteria:

44 Positive zonal wind and local maximum in excess of 30 m/s. We have modified Schiemann

45 et al.'s algorithm in several respects: ...

46   .

3. Meiyu Climatology

3.1. Algorithm

List version

For each day from 1 January 1951 to 31 December 2007 (20,819 total), the algorithm determines whether a frontal event is present or not inside the window of 105-123E and 20-40N, and if it exists returns its properties. In addition, it is observed that some days feature two frontal events. If a primary event is detected, the algorithm therefore checks for a secondary fit as well. The algorithm follows the subsequent checklist:

1. The maximum daily rainfall for each longitude is found. If there exists a 5°continuous chain of maxima (20 points in a row) exceeding 10 mm/day, we proceed to step 2 and attempt a fit. Otherwise, the day is thrown out.

2. A weighted least-squares linear fit of the *latitudes* of the maxima is attempted, using the intensity of the maxima as weight.

3. A recursive algorithm converges on a best estimate. In each iteration, we find a new set of maxima within k degrees of the previous best fit line, and again repeat the weighted linear fit in step 2. k is progressively decreased with each iteration.

4. Using our final best estimate from step 3, we define the "quality score" Q as the fraction of total daily precipitation that falls within 5 degrees of this fit line.

5. As mentioned, we check for a secondary front. We remove all precipitation within the primary front and again apply the front criterion in step 1 to the leftover rainfall map. If passed, steps 2-4 are repeated to find a best estimate for a secondary front.

66   6. If a secondary front is found, two additional quality scores Q_1 and Q_2 are determined.

67 Q_1 is defined as the fraction of rainfall contained in the primary front *after removing all*

68 *rainfall associated with the secondary front.* Likewise Q_2 is the Q score of the second front

69 after removing all rainfall from the primary front.

70   In some cases, a fit will be achieved, but its quality will be too poor to include in our

71 statistics. To check for this scenario, we use the quality scores Q, Q_1 and Q_2, and the

72 "Taiwan fraction" (TW), defined as the percentage of daily rainfall that falls on the island

73 of Taiwan. If $TW > 20\%$, the day is thrown out. Such days are dominated by a local

74 storm reaching Taiwan and rarely exhibit a strong front. Subsequently there are two ways

75 a day may be included:

76   1. if $Q > .6$, the day is included in our statistics. If Q_2 also is greater than .6, the day

77 will be classified as a double front day.

78   2. If $Q < .6$, a day can only be included if both Q_1 **and** $Q_2 > .6$. In such cases, the

79 quality of fit is initially obscured by the presence of multiple fronts. We classify the day

80 as a double front day.

81   In practice, days with secondary fronts constitute a small fraction of all days ($> 5\%$)

82 but are more common during certain seasons.

83 **Paragraph version**

84   For each day from January 1 1951 to December 31 2007 (20,819 days at all) we determine

85 whether there is a frontal event, whether there is an additional secondary front, and the

86 characteristics of each. To detect a front, we find the maximum daily rainfall at each

87 longitude inside the window 105-123°E and 20-40°N. If a 5°continuous chain of maxima

88   exceeds 10 mm/day, we seek a fit; otherwise the day is discarded. The fitting algorithm

89   performs a linear least-squares fit of the *latitudes* of each of the maxima, weighted by

90   the intensity of the maximum. Next, we use a recursive fit wherein we find a new set

91   of maxima, requiring that they be within n degrees of the previous best fit line. n is

92   progressively decreased to tighten the window and converge on an optimal fit. Given this

93   fit, we can calculate a quality score Q, which is the percentage of total rainfall in our

94   window that falls within 5 degrees of our best fit line. A score of $Q > .6$ constitutes a

95   good score, as further explained below.

96   In addition, we determine from observation that some days feature two separate bands

97   of strong rainfall. We would like to include such events. Therefore, after fitting a primary

98   event, we check for a secondary event by removing the rainfall associated with the first

99   best fit line, and then repeating all of the steps of the previous paragraph. If a secondary

100   event is detected, we may define two extra quality scores Q_1 and Q_2, where Q_1 is the

101   percentage of rainfall within *after removing rainfall associated with the secondary fit*, and

102   Q_2 likewise is the Q score of the secondary fit after removing rainfall from the primary

103   fit.

104   Finally, in some cases our front criterion will be satisfied, but we are not able to achieve

105   a good fit. We use the quality scores Q, Q_1 and Q_2 to check for this case, as well as

106   one additional metric, the "Taiwan fraction" (TW), defined as the percentage of daily

107   rainfall that falls on Taiwan. First of all, all days where $TW > 20\%$ are thrown out. Such

108   days are dominated by a local storm reaching Taiwan, and rarely exhibit a coherent front.

109   Subsequently there are two ways a day may be included:

110   1. if $Q > .6$, the day is included in our statistics. If Q_2 also is greater than .6, the day

111 will be classified as a double front day.

112   2. If $Q < .6$, a day can only be included if both Q_1 **and** $Q_2 > .6$. In such cases, the

113 quality of fit is initially obscured by the presence of multiple fronts. We classify the day

114 as a double front day.

115   In practice, days with secondary fronts constitute a small fraction of all days ($> 5\%$)

116 but are more common during certain seasons.

3.2. Statistics

117   Figure 1a reproduces a plot similar to Ding and Chan's 200x paper, but focusing on

118 eastern China. China receives a substantial fraction of its yearly precipitation outside of

119 summer, unlike a traditional monsoon circulation. Figure 1b shows a Hövmoller diagram

120 of the latitudes occupied by the Meiyu Front over all 57 years, including both primary and

121 secondary events, with a 5-day and 2°smoothing. Frontal events are found throughout

122 the year, with occurrence minimizing in January (10%) and maximizing in late June

123 (80%). However, it can be seen that mean rainfall and Meiyu occurrence are not entirely

124 equivalent. For instance, the August peak in southern China rainfall (about 20°N) does

125 not correspond to a surge in Meiyu events. Other known features of East Asian rainfall

126 are reproduced, such as the spring persistent rains beginning in March.

127   As pointed out in *Biasutti et al.* [2011], the statistics of rainfall incurrence are dependent

128 on the sampling interval. The intensity of storms likely remains relatively fixed, whereas

129 their frequency increases significantly. This view is confirmed by decades of observation

130 studies such as *Murakami and Huang* [1984], which find that frontal rainfall consists of a

131 string of mesoscale convective systems (MCS) separated by calm skies.

132 We focus on several periods of particular behavior:. These correspond to Ding and

133 Chan's ... Table 1 shows the mean characteristics of fronts in each of these periods and

134 their variance.

135 We test for the existence of statistically significant differences between 1951-1979 and

136 1980-2007 for each of the time periods mentioned above.

4. Preferred jet positions

137 -¿ The westerly jet and rainfall are argued to covary on paleoclimate timescales [*Na-*

138 *gashima et al.*, 2011][*Nagashima et al.*, 2013].

139 Monthly changes in the position of the jet have previously been reported in *Schiemann*

140 *et al.* [2009], and we do not repeat them here. It is worth noting that the pre-Meiyu in

141 May corresponds to a time of great jet variability, whereas June features a discernible but

142 meandering jet, and the post-Meiyu corresponds to very low variability in jet position

143 during July and August.

144 Finally, we use our knowledge of daily Meiyu positions to isolate preferred configurations

145 for different dates, as well as probability distributions of the tropospheric jet associated

146 with each configuration. If a robust change in mean jet progression is detected, we may

147 be able to isolate a corresponding shift in Meiyu distribution that may have previously

148 gone unnoticed due to extreme temporal variability in the data.

149 We first attempt to define a transition date from spring to summer behavior in the

150 jet database, and equivalently from Meiyu Season to post-Meiyu in our new catalog.

Preliminary evidence suggests a long-term perturbation in mean jet path in East Asia from the 1960s to present with later onset of summer jet and shorter total duration of summer jet. In our Meiyu database it is more difficult to extract an exact transition date due to high-frequency variability in space and time. However, we observe an apparent shift in the timing of northward progression of the Meiyu Front between 1951-1970 and 1988-2007. If both databases demonstrate a robust decadal shift, they may provide an explanation for the anecdotal South Wet-North Dry pattern of rainfall change.

5. Covariance of jet and Meiyu anomalies

6. Dynamics

The covariance of Meiyu front positions and tropospheric jet latitudes previously demonstrated also clarifies a dynamical reason for their seasonality. As shown, Meiyu season consists of intense rainfall from June 1st to July 1st with a shift in latitude of almost 10 degrees over the course of that month. After In the climatological mean, *Chen and Bordoni* [2014] demonstrated that the Meiyu front exists primarily due to forced mechanical convergence by the Tibetan Plateau upstream. The season of peak rainfall and peak Meiyu frequency corresponds directly to the period when the westerly jet is impinging on the Tibetan Plateau upstream. When the jet moves further north to its preferred summer position, which occurs just north of the Tibetan Plateau, it is no longer deflected and the front is significantly weaker, and we transition to a preferred double-front state as seen in figure 1b.

7. Conclusion

Since the behavior of the jet is coupled to global climate variability, our work holds the promise of attributing the regional rainfall trend in China to global-scale change.

-¿ Existing templates for precipitation changes under warming ([*Held and Soden*, 2006][*Lintner and Neelin*, 2007][*Chou et al.*, 2009]) are not easily applied to the East Asian monsoon

References

Biasutti, M., S. E. Yuter, C. D. Burleyson, and A. H. Sobel (2011), Very high resolution rainfall patterns measured by TRMM precipitation radar: seasonal and diurnal cycles, *Clim. Dyn.*, *39*(1-2), 239–258, doi:10.1007/s00382-011-1146-6.

Chen, J., and S. Bordoni (2014), Orographic Effects of the Tibetan Plateau on the East Asian Summer Monsoon: An Energetic Perspective, *J. Climate*, *27*(8), 3052–3072, doi: 10.1175/JCLI-D-13-00479.1.

Chou, C., J. D. Neelin, C.-A. Chen, and J.-Y. Tu (2009), Evaluating the rich-get-richer mechanism in tropical precipitation change under global warming, *J. Climate*, *22*(8), 1982–2005, doi:10.1175/2008JCLI2471.1.

Ding, Y., and J. C. L. Chan (2005), The East Asian summer monsoon: an overview, *Meteorol. Atmos. Phys.*, *89*(1-4), 117–142, doi:10.1007/s00703-005-0125-z.

Held, I., and B. Soden (2006), Robust responses of the hydrological cycle to global warming, *J. Climate*, *19*(21), 5686–5699.

188 Kosaka, Y., S.-P. Xie, and H. Nakamura (2011), Dynamics of Interannual Variabil-

189   ity in Summer Precipitation over East Asia *, *J. Climate*, *24*(20), 5435–5453, doi:

190   10.1175/2011JCLI4099.1.

191 Liang, X., and W. Wang (1998), Associations between China monsoon rainfall and tro-

192   pospheric jets, *Q. J. R. Meteorol. Soc.*, *124*(May), 2597–2623.

193 Lintner, B., and J. D. Neelin (2007), A prototype for convective margin shifts, *Geophys.*

194   *Res. Lett.*, *34*(5), L05,812, doi:10.1029/2006GL027305.

195 Murakami, T., and W.-G. Huang (1984), Orographic effects of the Tibetan Plateau on

196   the rainfall variations over central China during the 1979 summer, *J. Meteorol. Soc.*

197   *Japan*, *62*(6), 895–909.

198 Nagashima, K., R. Tada, A. Tani, Y. Sun, Y. Isozaki, S. Toyoda, and H. Hasegawa (2011),

199   Millennial-scale oscillations of the westerly jet path during the last glacial period, *J.*

200   *Asian Earth Sci.*, *40*(6), 1214–1220, doi:10.1016/j.jseaes.2010.08.010.

201 Nagashima, K., R. Tada, and S. Toyoda (2013), Westerly jet-East Asian summer monsoon

202   connection during the Holocene, *Geochemistry, Geophys. Geosystems*, *14*(12), 5041–

203   5053, doi:10.1002/2013GC004931.

204 Sampe, T., and S.-P. Xie (2010), Large-Scale Dynamics of the Meiyu-Baiu Rain-

205   band: Environmental Forcing by the Westerly Jet, *J. Climate*, *23*(1), 113–134, doi:

206   10.1175/2009JCLI3128.1.

207 Schiemann, R., D. Lüthi, and C. Schär (2009), Seasonality and Interannual Variability

208   of the Westerly Jet in the Tibetan Plateau Region, *J. Climate*, *22*(11), 2940–2957,

209   doi:10.1175/2008JCLI2625.1.

210 Yatagai, A., K. Kamiguchi, O. Arakawa, A. Hamada, N. Yasutomi, and A. Kitoh (2012),

211 APHRODITE: Constructing a Long-Term Daily Gridded Precipitation Dataset for Asia

212 Based on a Dense Network of Rain Gauges, *Bull. Am. Meteorol. Soc.*, *93*(9), 1401–1415,
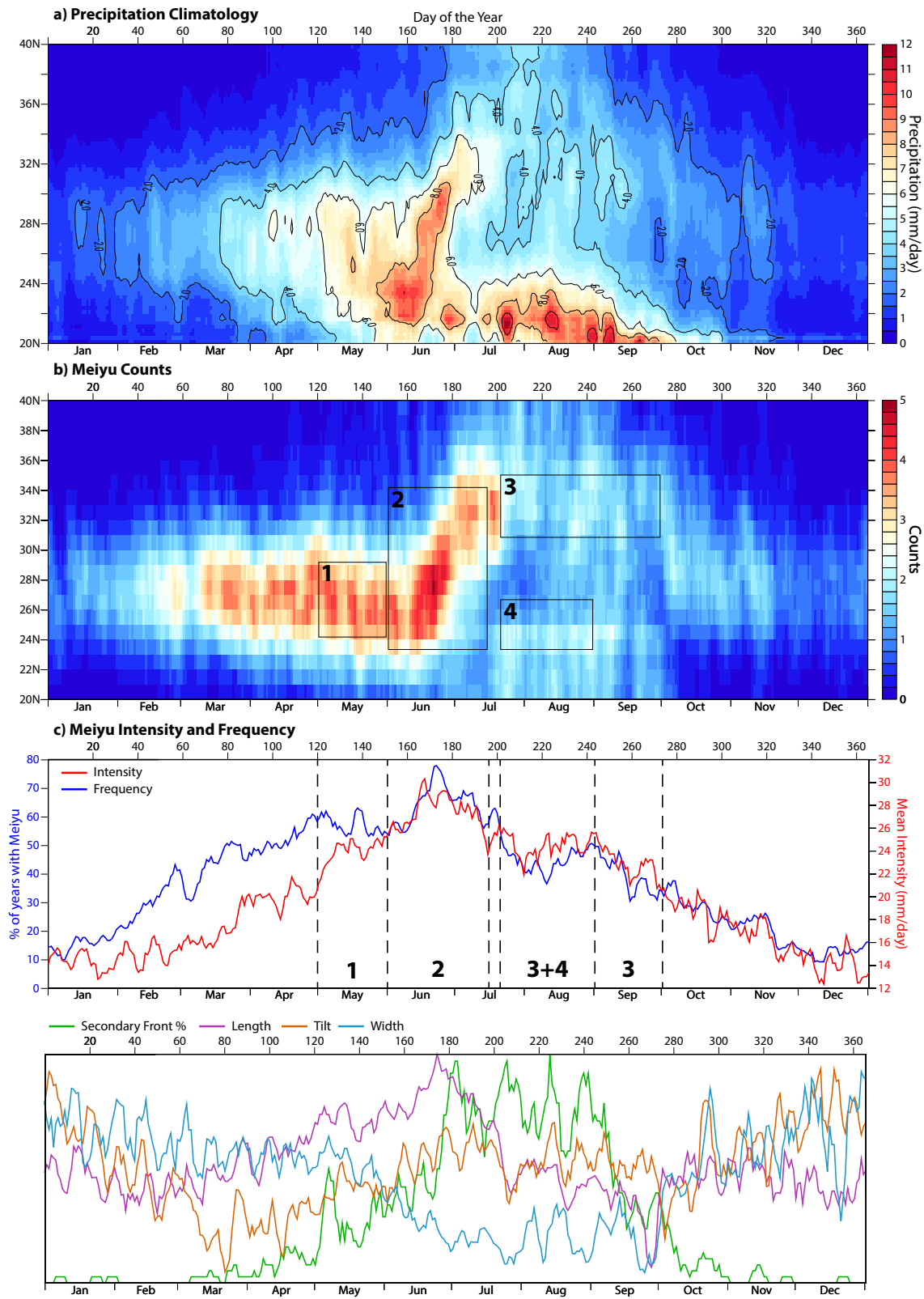
213 doi:10.1175/BAMS-D-11-00122.1.

Figure 1. Climatology of the Meiyu Front, 1951-2007. 1) Pre-Meiyu 2) Meiyu 3) Cyclone season in Southern China 4) Storms advected by summer jet